Structural remodeling of peripheral taste neurons is fast and independent of taste cell turnover

Zachary D. Whiddon[1], Jaleia Marshall[1], David Alston[1], Aaron McGee[1], and Robin F. Krimm[1#]

[1]Department of Anatomical Sciences and Neurobiology, University of Louisville School of Medicine, Louisville, KY 40202

*These authors contributed equally to this work

[#]Correspondence to: Dr. Robin Krimm, MDR building, room 405B, 511 S. Floyd Street, Louisville, KY 40202

Key Words: taste, geniculate neuron, morphology, afferent, tongue

No. of Figures: 7
No. of Supplemental Figures: 1
No. of supplemental Tables: 0
No. of supplemental Movies: 1

ABSTRACT

Taste bud cells are constantly replaced in taste buds as old cells die and new cells migrate into the bud. The perception of taste relies on new taste bud cells integrating with existing neural circuitry, yet how these new cells connect with a taste neuron is unknown. Do taste neurons remodel to accommodate taste bud cell renewal? If so, how much of the taste axon structure is fixed and how much remodels? We measured the motility and branching of individual taste arbors (the portion of the axon innervating taste buds) over time with two-photon *in vivo* microscopy. Terminal branches of taste arbors continuously and rapidly remodel within the taste bud. This remodeling is faster than predicted by taste bud cell renewal, with terminal branches added and lost concurrently. Surprisingly, ablating new taste cells with chemotherapeutic agents revealed that remodeling of the terminal branches of taste arbors does not rely of the renewal of taste bud cells. Although the arbor structure remodeling was fast and intrinsically controlled, no new arbors were added, and few were lost over 100 days. Taste neurons maintain a stable number of nerve arbors that are each capable of high-speed remodeling. Arbor structural plasticity would permit arbors to locate new taste bud cells, while stability of arbor number could support constancy in the degree of connectivity and function for each neuron over time.

Introduction

The replacement of cells in the taste bud was discovered more than fifty years ago ago (Beidler and Smallman, 1965). In fact, cells within a taste bud are one of the fastest renewing cell populations in the body, with an average lifespan of 10 days (Beidler and Smallman, 1965; Farbman, 1980; Lindemann, 2001). Taste bud cells transduce chemical stimuli in the oral cavity, and transmit it to the axons of ganglion neurons, which carry this information to the brain. Each time a taste bud cell dies, the axon of a taste ganglion neuron (taste axons) must connect with a new taste bud cell if it is to maintain functional integrity (Kumari et al., 2017; Lee et al., 2017). This process by which taste axons disconnect from one taste bud cell and reconnect with another is unclear, but could involve structural remodeling of the nerve fiber. Alternatively, taste bud cells could migrate to the nerve fiber, making axon remodeling unnecessary. Equally, unclear is whether this process of repeated reconnections is disrupted by factors that disrupt taste bud cell turnover (e.g. chemotherapies). Lastly, given this constant formation of new connections it is unclear how/if this system maintains functional consistency over time (e.g., sweet is always sweet).

Taste neurons are pseudo-unipolar sensory neurons with a single axon that branches to project both centrally and peripherally (Yarmolinsky et al., 2009; Zaidi and Whitehead, 2006). The peripheral axons of taste neurons vary considerably in structure due to differences in the number of branch points within the tongue muscle, the lamina propria and within the taste bud (Huang et al., 2021). This structural variation across taste neurons dictates their connectivity and likely their function. What is unclear is whether this variation exists because there are several types of taste peripheral neurons that differ in

structure. Instead, taste neuron morphology could be dictated by structural plasticity such that the structure of individual neurons represents snap-shots in time of differing plastic states (Anderson and Larson, 2019; Dvoryanchikov et al., 2017; Ohman and Krimm, 2021; Zhang et al., 2019),

Here we examined the structure of peripheral taste axons using *in vivo* two-photon microscopy to determine how taste neuron structure changes over time. We discovered that taste axon structure inside the taste bud remodels surprisingly quickly and this remodeling is intrinsically regulated. We also discovered the number of arbors each taste axon has is a stable feature of neurons. While the remodeling portions of the taste axon illustrate the cellular movements required for a taste axon to connect with new taste bud cells over time, stable portions of the axon could support functional stability over time.

Results

Acute *in vivo* imaging reveals axonal structural plasticity

To determine whether axon structure in the peripheral taste system is fixed or remodels over time, we developed an *in vivo* preparation to image the portion of the taste neuron's axon that terminates in the taste bud (arbors). The arbors of taste neurons enter taste buds in the epithelium. On the front two-thirds of the mammalian tongue, taste buds are housed in epithelial structures called fungiform papillae, which are easily accessible for imaging in live animals (Miller and Reedy, 1990). Within taste buds, arbors form a dense plexus with many overlapping branches (Ohman-Gault et al., 2017; Wilson et al., 2022). We used a sparse-labeling strategy to express tdTomato in a small number of taste neurons so that individual arbors could be distinguished (Huang et al., 2021). In this preparation, fewer than five labeled arbors were labeled with tdTomato per fungiform

taste bud and many taste buds did not contain any labeled arbors. Individual arbors were imaged using two-photon laser scanning microscopy (Figure 1A).

Individual arbors were imaged up to a depth of 70 microns to capture the entire arbor, as well as a portion of the axon beneath the taste bud. To estimate the frequency of structural plasticity for these axons, first we imaged the same arbors once per hour for a 6 h period (n=36). We found that arbor structure within the lamina propria (Figure 1A, purple dotted-line) of the fungiform papilla core was stable (Figure 1B, yellow box). Many of the terminal branches of arbors within the taste bud (Figure 1A, green dotted line) displayed structural changes in as quickly as a few hours after the initial imaging session (Figure 1B, red box). Among the 36 arbors imaged, 24 changed their number of terminal branches in a 6 h window by adding and/or subtracting small terminal branches.

To determine whether the very low excitation power (<51 mW) used for imaging induced evident photobleaching, we imaged a new group of arbors (n=13 from two mice) using identical acquisition parameters every hour for 6 h and compared the fluorescence intensity across image stacks (z-max intensity projections) for the first and last timepoints. We did not observe a significant decrease in average ($t(12) = -1.78$, $p = 0.076$) or maximum ($t(12) = -1.78$, $p = 0.380$) fluorescence intensity despite imaging these structures repeatedly (Figure 1C). Thus, this imaging approach was suitable for acute *in vivo* imaging of individual taste neuron arbors and demonstrates that arbors of taste neurons display high-speed structural remodeling.

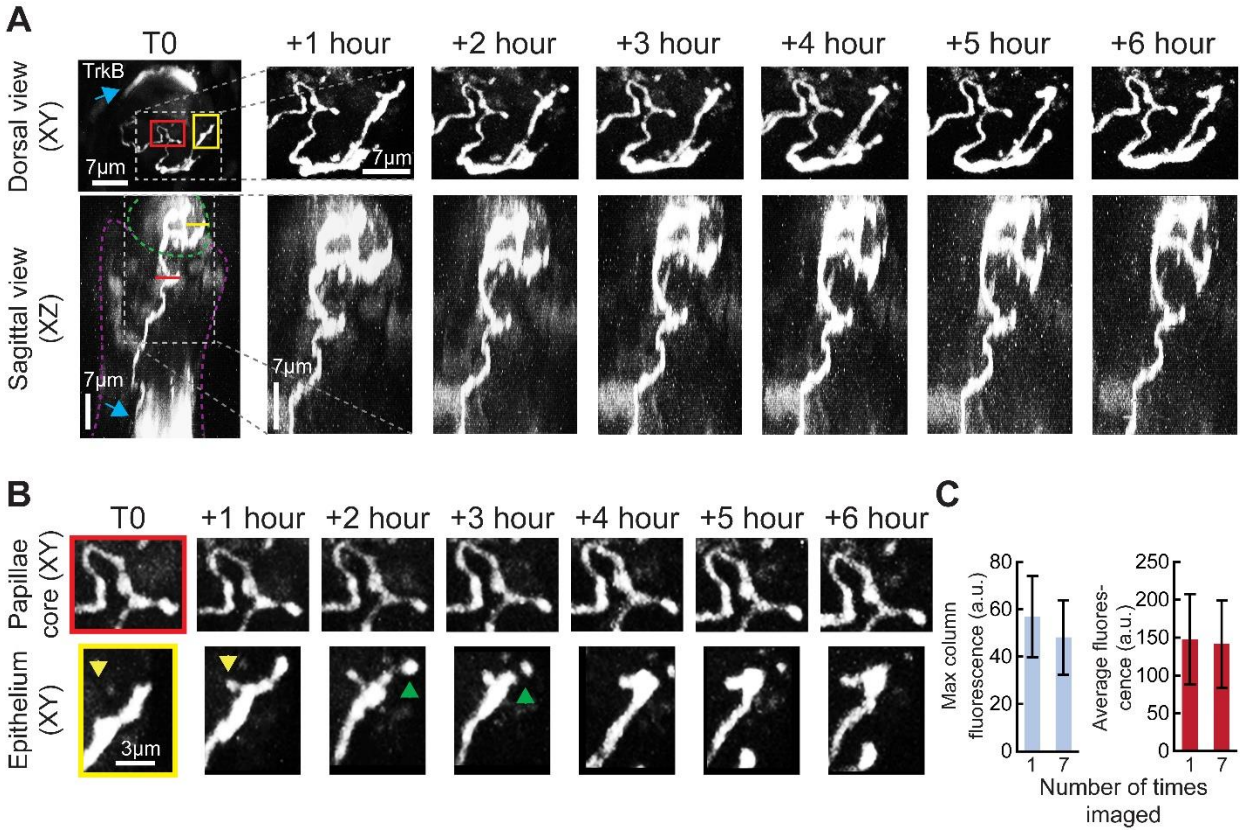

Figure 1. Intravital imaging of taste neurons in fungiform papillae. Example of a fungiform papilla with a single labeled receptive arbor illustrating the small-scale changes that can be seen within 6 hours. (**A**) Top and bottom rows show dorsal (XY) and sagittal (XZ) views of an arbor within a fungiform papilla every hour over a 6 h period. Some keratinocytes were also labeled (Liu et al., 2012; Tang et al., 2017) (cyan arrow). After T0, images for each consecutive timepoint are enlarged to show only the labeled arbor. At T0, the taste bud is outlined in a green dotted line, and the connective tissue core of the papilla is outlined in magenta. (**B**) High-magnification view (XY projection) of structural features of the arbor within the papilla core (red box) and taste bud (yellow box). The branch ending inside the taste bud bifurcated after 1 h and then reverted to a single branch ending after 4 h (yellow and green arrowheads). The portion of the arbor in the papilla core did not change across the 6 h imaging window. (**C**) Comparison of average and maximum fluorescence (mean ±SD), using regions of interest around receptive arbors, in max intensity z-projections of arbors imaged every hour for 6 h.

Chronic *in vivo* imaging requires a fungiform papillae map

Next, we examined axonal structural plasticity over days. Reliably identifying the same taste buds across imaging sessions was critical for chronic imaging experiments.

To identify the same taste buds over days or weeks, we combined our approach for sparse labeling of taste neurons (*Ntrk2*^{CreER} :tdTomato) with transgenic mice that express green fluorescent protein (GFP) in taste buds (*Sox2*^{GFP}: Okubo et al., 2006). When viewed at low-magnification, GFP expression on the anterior tongue surface revealed a unique taste bud pattern for each mouse (Figure 2A) This provided a set of fiduciary marks used to locate the same taste buds and arbors repeatedly over time. Three taste buds in the example papillae map contained labeled arbors; they are shown at high magnification 24 h apart (Figure 2B). No other fungiform taste buds viewed in this field contained labeled arbors because of the sparseness of genetic labeling of taste neurons (Figure 2A, taste buds with no box).

Taste bud cells have an average lifespan of 10 days (Beidler and Smallman, 1965). Given this rate of taste bud cell turnover, we investigated the structural plasticity of arbors every 12 h for 10 days. In five mice, we observed the same 31 taste buds and 60 labeled arbors 21 times over 10 days. Among these arbors, four were lost during this period, and none were added. One taste bud lost GFP expression in the epithelium, but the arbor remained, consistent with taste bud loss due to aging (Liebl et al., 1999; Patel and Krimm, 2010). Examination of a single-labeled arbor at the beginning and end of the 10-day experiment illustrates that arbor structure in the papillae core was stable, whereas arbor structure in the epithelium was plastic (Figure 2C).

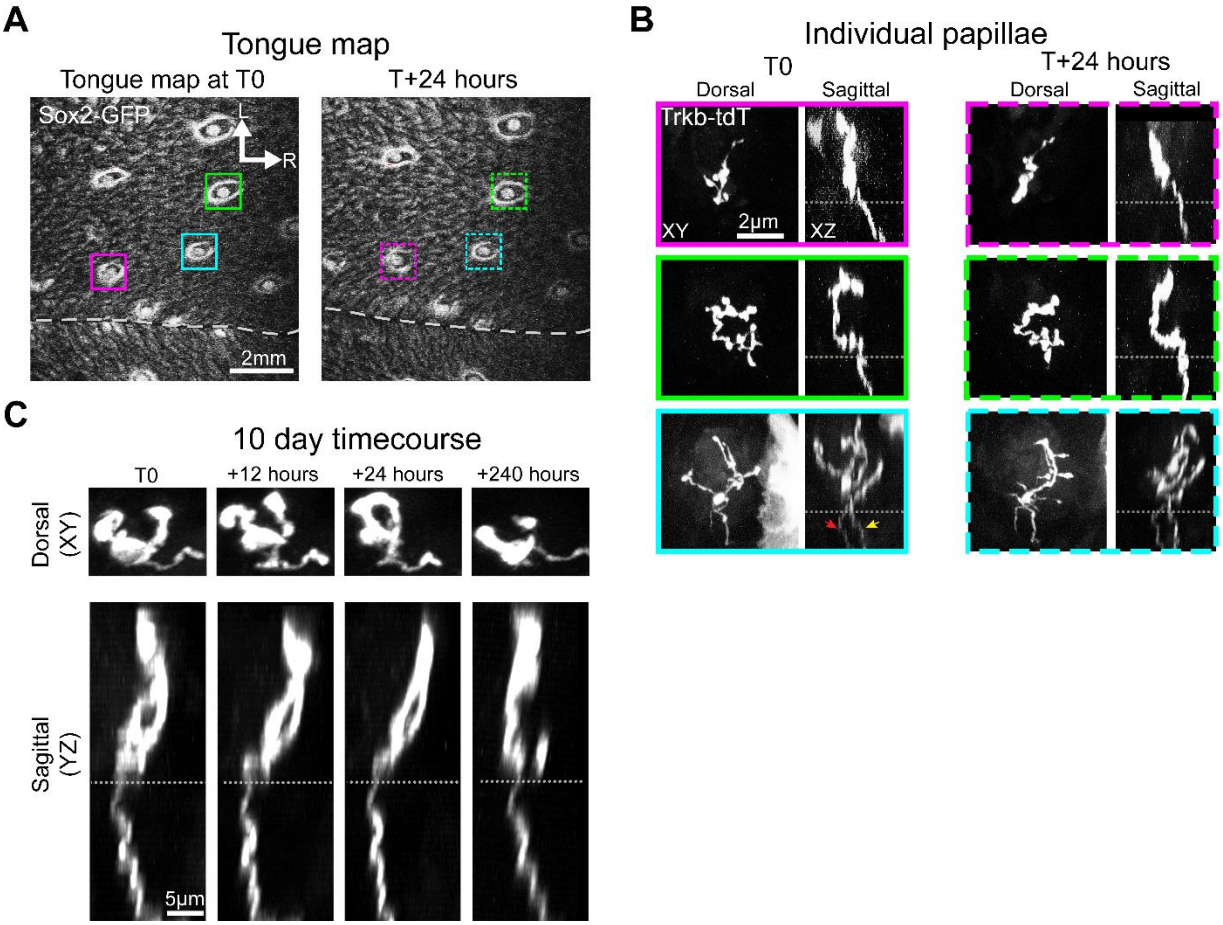

Figure 2. Chronic intravital imaging using a papillae map. (**A**) Sox2-GFP expression in the anterior tongue epithelium illustrating a papillae map. Papillae with labeled arbors are indicated by solid boxes at T0 and dashed boxes 24 h later. The tongue midline is indicated with a white dashed line, and rostral (R) and lateral (L) directions are indicated by white arrows. (**B**) High-magnification micrographs of TrkB-tdTomato-labeled nerve arbors in each of the three papillae indicated from the map. The first column shows the XY (dorsal) plane, which is parallel to the tongue surface, and the XZ plane is shown in the adjacent column. Gray dashed lines in the z-plane images illustrate the bottom of the taste bud. The papillae outlined in magenta and green have a single labeled arbor, and the papilla outlined in cyan has two separate labeled arbors (yellow and red arrows). Micrographs outlined in dashed lines show high-magnification views of the same papillae 24 h later. Some changes to each arbor structure can be seen during this time within the taste bud but not within the papillae core. (**C**) Receptive arbors were imaged every 12 h for 10 days, and an example arbor is shown at the initial timepoint (T0) as well as 12, 24, and 240 h later.

Terminal branches remodel rapidly and continuously over 10 days

Taste neuron arbors synapse with taste bud cells (Kinnamon et al., 1988; Romanov et al., 2018; Vandenbeuch et al., 2015). Many connections between taste neuron arbors and taste bud cells occur on terminal branches (Kinnamon et al., 1988). If the turnover of taste bud cells regulates arbor structure, then terminal branches are likely to remodel as taste bud cells die and/or new cells enter the taste bud. Arbors form connections with an average of 1.6 taste bud cells (Kinnamon et al., 1988). If new terminal branches are added and lost as a means of connecting with new taste bud cells, then most arbors should add or lose roughly one terminal branch over 10 days, and some arbors are likely to remain stable.

In five mice, we imaged 31 taste buds containing a total of 60 arbors. However, taste buds with three or more labeled arbors were not quantified because we could not distinguish arbors when branches intermingled. We identified 26 individual arbors from 21 different taste buds that were distinguishable at all timepoints and quantified their terminal branches every 12 h (Figure 3A-B, video 1). All quantified arbors added and lost multiple terminal branches during within 10 days (Figure 3B-C). In 43% of arbors, a terminal branch was lost or added within the first 12 h, and 100% of arbors gained or lost a branch within the first 4.5 days (108 h, Figure 3D). For the 30 arbors imaged every 12 h for at least 4 days, one terminal branch was added or lost every 16.8 ± 1.1 h. This anatomical plasticity was much faster than predicted based on the rate of taste bud cell turnover. Thus, terminal branches do not appear to be added for the primary purpose of connecting with a new taste bud cell or lost solely as a mechanism for disconnecting from dying taste bud cells.

Given the high rate of terminal branch addition and removal, we suspected that we could be underestimating the rate of change if some terminal branches were both gained and lost within the 12 h intervals between imaging sessions. To test this possibility, we imaged every 4 h for a 12 h period. For this image set (n = 33 arbors), an average of one terminal branch was added or lost every 6.8 ± 0.9 h, which was a significantly faster rate of change than the one obtained when arbors were imaged every 12 h (16.8 h; Figure 3E, $U = 276$, $p < 0.001$, Mann-Whitney U). These results indicate that imaging every 12 h underestimates the rate of terminal branch change. To verify the accuracy of this rate of terminal branch change, we compared arbors imaged every 4 h to arbors imaged every hour for 6 h (n = 36) and found no significant difference in the rate of terminal branch gain/loss (1 h rate: 5.5 ± 0.8 h; 4 h rate, 6.8 ± 0.9 h; $U = 423.5$, $p = 0.29$) (Figure 3E). Thus, we conclude that accurately describing changes in terminal branch number requires sampling arbor structure every 4 h. However, given the high rate of terminal branch addition and loss, we also sought to determine whether two-photon exposure influences the rate of terminal branch addition/loss. We compared arbors imaged twice in 6 h with arbors imaged seven times over the same amount of time (Figure 3F). There was no difference in the rate of change in terminal branch number over the 6 h period between these two sets of arbors, indicating that image collection does not influence the rate at which terminal branches are added and lost.

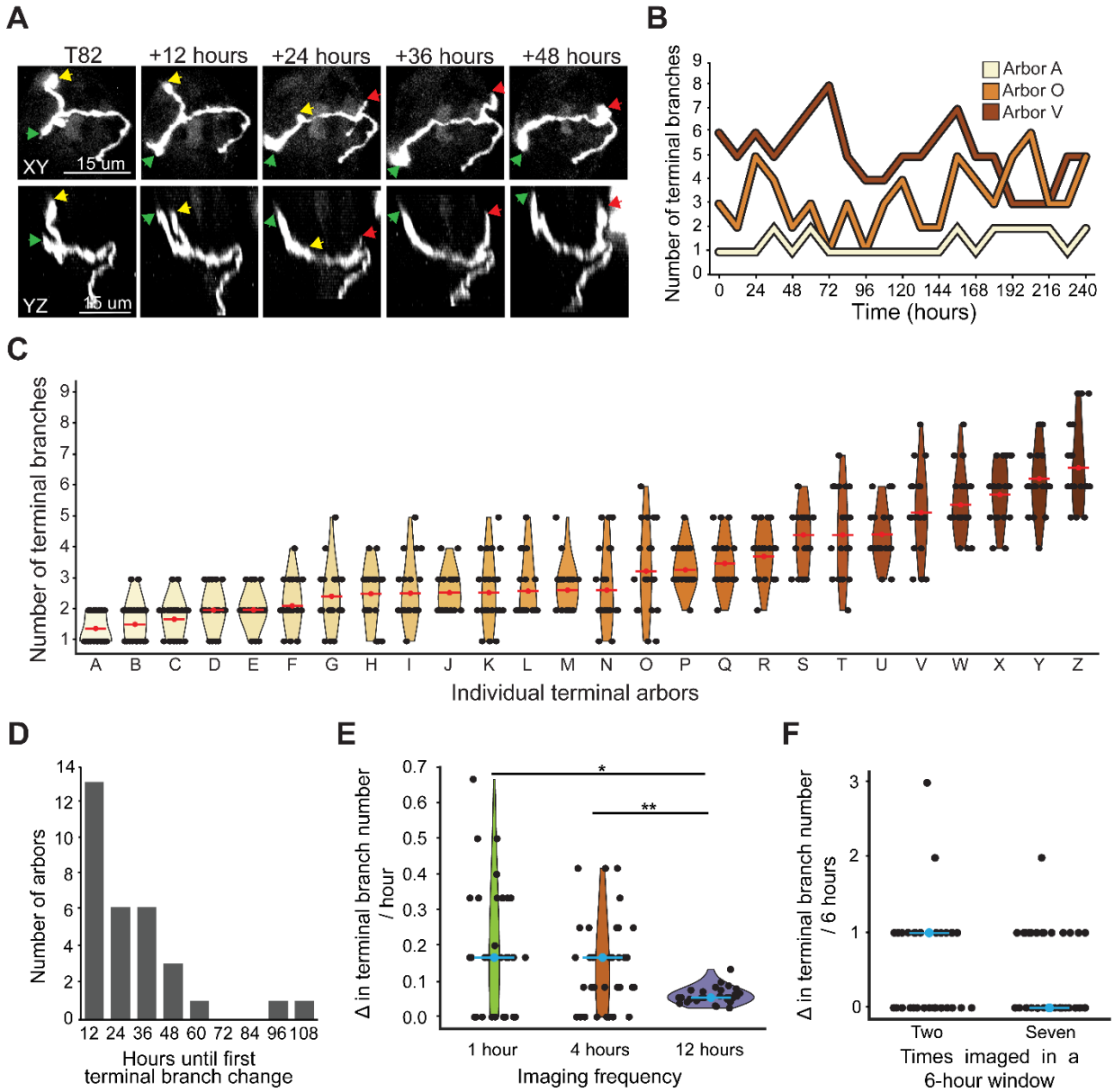

Figure 3. Terminal branches are continuously and rapidly remodeled. (**A**) Example arbor shown every 12 h over 2 days (for the full 10 days see Figure 3, see supplementary movie 1 for full 10 days). Terminal branches labeled with green and red arrowheads extended during this period, while the terminal branch labeled with a yellow arrowhead retracted. (**B**) Number of terminal branches every 12 h for three arbors across the 10-day imaging window. (**C**) Violin plots for 26 (A-Z) individual arbors showing the distribution of terminal branch number during the 10-day imaging window. Arbors are arranged in ascending order of average terminal branch number (red dot and bar) across 10 days. (**D**) Amount of time until the first gain or loss of a terminal branch. All arbors added or lost a terminal branch within 108 h. (**E**) Violin plots showing rates of change in terminal branch number per hour for three different sampling frequencies: 1, 4, or 12 h. Median values are indicated with cyan dots and bars (Single asterisk $p<0.05$, double $p<0.001$). (**F**) Rate of change in terminal branches over 6 h for arbors imaged twice compared with arbors imaged seven times. Median values are indicated with cyan dots and bars.

197

Gain/loss of terminal branches is not regulated by taste bud cell turnover

If arbors add new branches to connect with new taste bud cells, then altering the rate of new cell entry would be expected to alter terminal branch dynamics. To test the hypothesis that taste neuron remodeling is dependent on the addition of new taste bud cells we prevented new cells from being added to taste buds by blocking Hh-signaling. Administering LDE225 (trade name Sonidegib) (Figure 4A) stops new taste cells from differentiating and entering taste buds (Castillo et al., 2014; Castillo-Azofeifa et al., 2017; Ermilov et al., 2016; Kumari et al., 2017, 2015; Lu et al., 2018) (Figure S1). This is a chemotherapeutic agent used to treat basal cell carcinoma and is associated with loss of

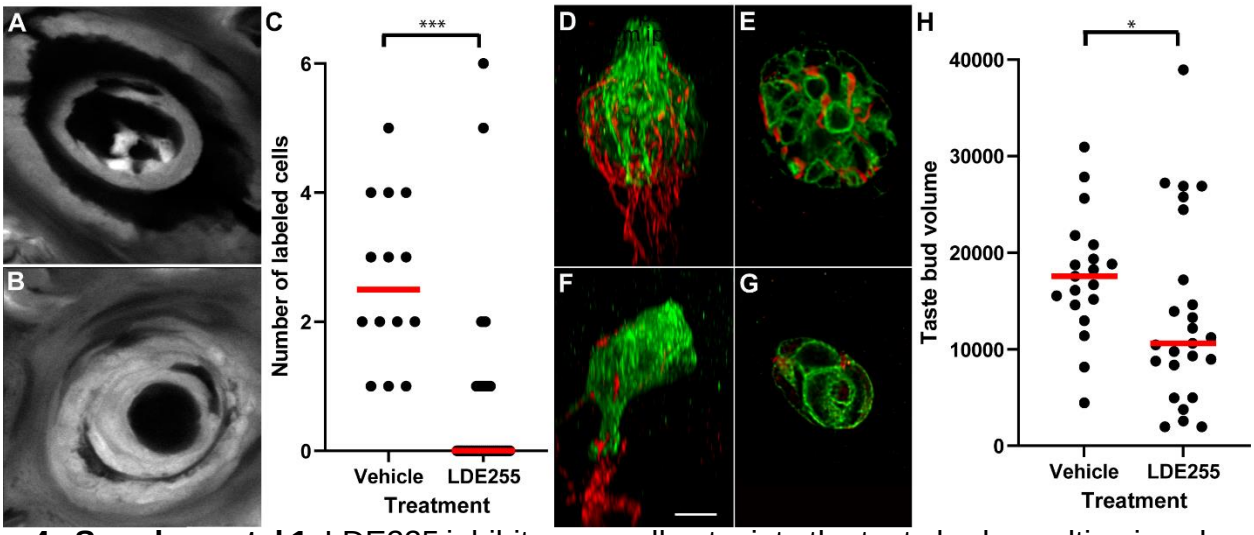

Figure 4 - Supplemental 1. LDE225 inhibits new cell entry into the taste bud, resulting in volume reduction by day 10. **A-C)** A subset of epidermal precursor and/or stem cells expressing K14-CreER:tdTomato were labeled with a single dose of tamoxifen immediately preceding 10 days of treatment with vehicle (**A**) or LDE225 (**B**). On day 10, LDE255-treated mice had fewer labeled cells in taste buds than vehicle-treated mice (**C**). Specifically, 27 of 40 taste buds completely lacked new labeled cells following LDE255 treatment, while all those examined had some labeled cells following vehicle treatment. (**D-H**) Whole mounts of the lingual epithelium were labeled for taste buds (green) and neurons (Phox2b-tdTomato, red) following 10-day of treatment with vehicle (**D** z-plane, **E** x-y plane) and LDE225 (**F** z-plane, **G** x-y plane) tongues. (**H**) Taste bud volumes were smaller following 10 days of LDE225 compared with vehicle controls. *$p \leq 0.05$, ***$p \leq 0.001$.

taste by patients receiving treatment (Jacobsen et al., 2016; Kumari et al., 2015; Lacouture et al., 2016; Tang et al., 2012).

We treated mice with LDE225 (n=4) or vehicle (n=2) for 10 days and imaged taste neuron arbors every 4 h for 12 h on days 6, 8, and 10. Over time, old taste cells continue to die and taste bud volume decreases (Castillo-Azofeifa et al., 2017) (Figure S1). However, arbors had similar rates of terminal branch change on each day of imaging ($H(30) = 29.5$, $p = 0.44$). Terminal branch gain/loss was similar between the LDE225 and vehicle groups ($U = 312$, $p = 0.61$) (Figure 4B). Thus, we conclude that preventing new cells from entering taste buds does not alter the rate of terminal branch remodeling.

We also examined how taste buds recover following treatment with LDE255. Many fungiform papillae recovered normal taste bud morphology, however some failed to recover and lacked Sox2 expression up to 40 days after treatment for 10 days with LDE225 (Figure 4C). Non-recovered papillae retained taste neuron innervation even in the absence of taste buds (Figure 4D). Surprisingly, we observed at least some remodeling of terminal branches in all papillae that lacked taste buds. Two example papillae with single labeled arbors are shown in Figure 4E. We conclude from these findings that the taste bud is not required for terminal branch remodeling of taste arbors.

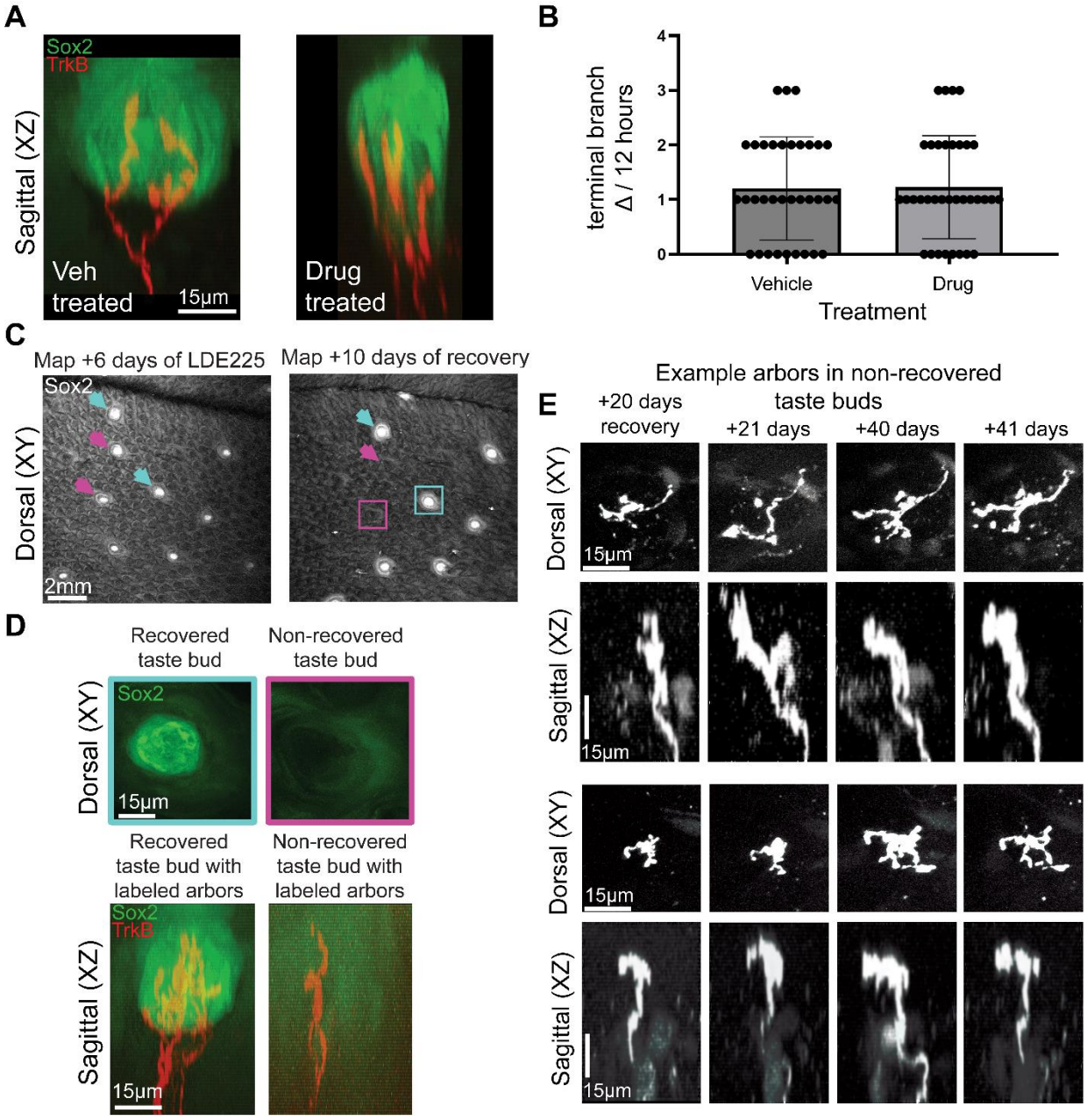

Figure 4. Terminal branch remodeling is not influenced by addition of new cells into the taste bud. (**A**) Example vehicle-treated and drug-treated taste buds after 8 days of treatment. (**B**) There was no difference in the rate with which terminal branches were gained/lost when taste bud cell turnover was halted (LDE225-treated mice) compared with normal conditions (vehicle-treated/untreated mice). (**C**) After LDE225 treatment, some fungiform papillae did not regain taste buds as determined by Sox2-GFP (magenta arrows and box). Two recovered taste buds are indicated with blue arrows and box. (**D**) Individual fungiform papillae with a taste bud had high levels of Sox2 expression, whereas papillae without a taste bud lacked cells with high levels of Sox2 expression. Papillae with both recovered and non-recovered taste buds retained taste neuron innervation. (**E**) Two papillae containing non-recovered taste buds with single-labeled arbors are shown 20, 21, 40, and 41 days after LDE225 treatment. Both arbors continued to remodel somewhat despite the absence of a taste bud.

Growth and retraction occur concurrently within the arbor

Some terminal branches displayed distinct morphologies as swellings on the tip of the terminal branch, as well as punctate swellings along the axon (Figure 5A). We suspected these features could be associated with remodeling, as both retraction bulbs and growth cones have been described in taste arbors (Zaidi et al., 2016). To determine if terminal branch swellings were associated with gain or loss of terminal branches, we examined 12 arbors from three mice that were imaged every 12 h for 10 days (n = 252 total timepoints). We observed 72 instances of swellings at the tip of the terminal branch and/or branch swellings long the branch. These terminal swellings along the axon were followed by retraction of the branch 86.1% of the time, whereas only 13.9% of terminal branches displayed terminal branch swelling without retracting (Figure 5B). Therefore, we conclude that terminal end swellings are often associated with retracting terminal branches (Figure 5A).

Since not all branch loss is associated with a retraction bulb, one possibility is that only those retractions with a retraction bulb occur when taste cells are lost. We examined the frequency of retractions which were associated with retraction bulbs to determine these retractions occurred at a rate consistent with branch retraction following the loss of connected bud cells. Retractions with retraction bulbs occurred at a frequency of once per 40 h and was also faster than the rate predicted by cell turnover. This finding indicates that branches retract for reasons other than loss of taste bud cells.

We next investigated whether retractions associated with retraction bulbs contributed to reduced arbor size by comparing the volume occupied by the arbor (convex hull; Figure 5C) and arbor length (Figure 5D) before and after terminal branch retraction.

Retraction of a single terminal branch did not alter total arbor size (Student's unpaired t-test, t=0.4515, df=74, p=0.65). These lost branches may represent a small percentage of the total branch length. Consistently, the average length of retraction for a single branch identified using end bulbs and beading was 14.1± 11.9 µm (Figure 5E), which was a small percentage of the mean total length of these arbors (79.2 ± 40.8 µm). In addition, branch elongation also commonly occurred in the arbor at another location concurrently with terminal branch retraction. Consistently, 21 of 38 arbors increased in total length while retracting a terminal branch. These opposing changes in branch length maintain arbor size over time.

Given that arbors add and lose terminal branches concurrently to maintain size, we wondered to what extent the total range of arbor complexity, measured as terminal branch number, changed in each arbor over 10 days. We observed that most arbors maintained a limited range of complexity over 10 days (Figure 5F), such that the minimum and maximum number of terminal branches for each arbor was correlated (Figure 5G, $R^2 = 0.698$, $p < 0.001$). Simple arbors (1-3 branches) did not become complex (more than 6 branches) within a 10-day window. Although large branch retractions also occurred frequently within 10 days, they occurred simultaneously with terminal branch formation, which limited the range of complexity for most arbors.

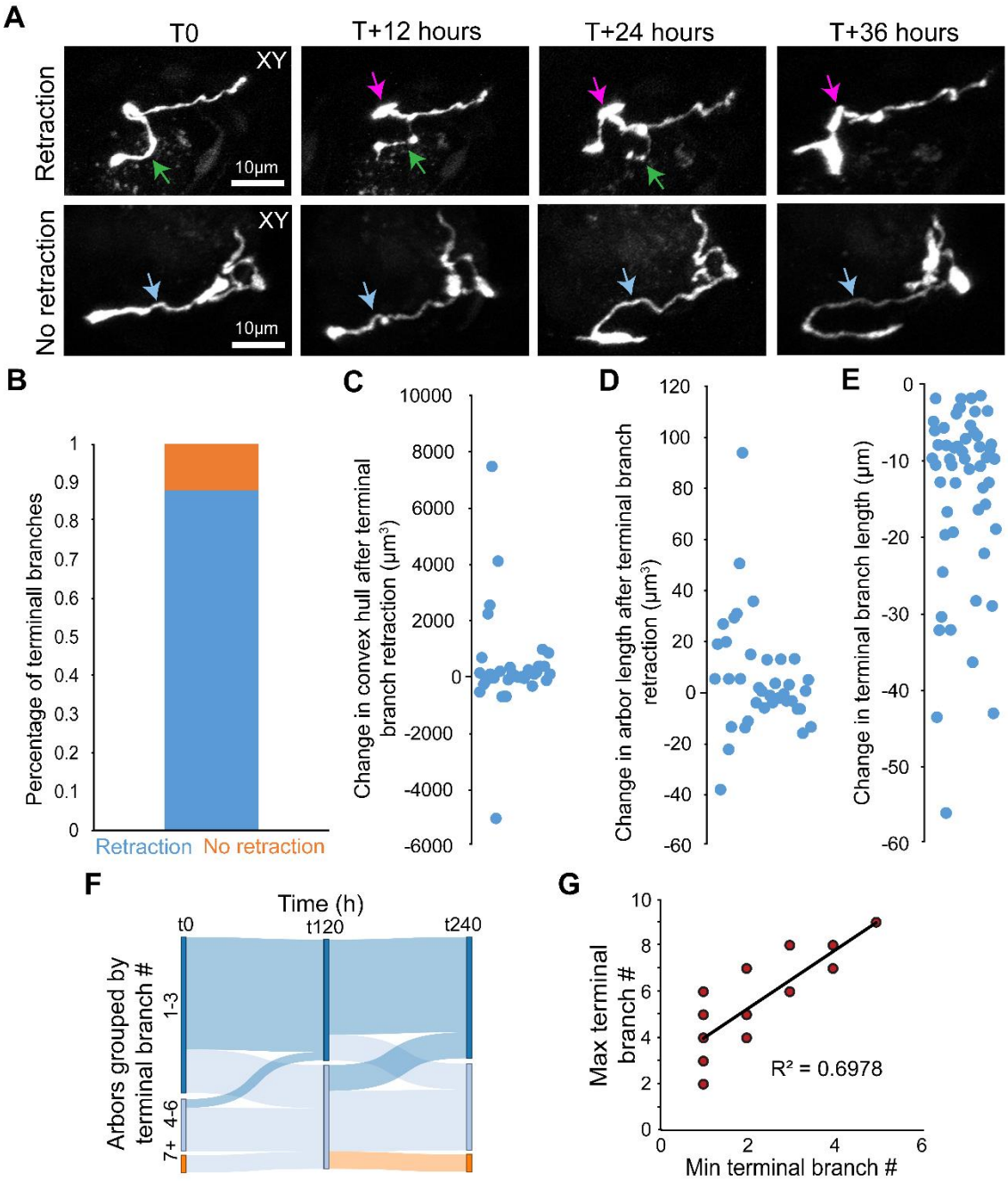

Figure 5. Morphologic changes predict terminal branch retraction but not change in arbor size. (**A**) Two example arbors shown across a 36 h window. In the top row, a terminal branch retracted after displaying a bulb at the tip of the ending and swellings within the branch (green arrow). A separate terminal branch on this same arbor extended (magenta arrow) in conjunction with terminal branch retraction. In the bottom row, a terminal branch displayed an end-bulb and swellings but did not retract (blue arrow); instead, it extended, indicating that the bulb may have been a growth cone. (**B**) Most terminal branches that displayed end-bulbs and swellings retracted at later timepoints (blue); however, a small portion did not retract (orange). (**C**) Change in convex hull after each terminal branch retraction. (**D**) Net change in total arbor length after each terminal branch retraction. (**E**) Change in terminal branch length. (**F**) Sankey diagram showing arbors grouped based on total number of terminal branches (1 to 3 = dark blue, 4 to 6 = light blue, 7+ = orange). Most arbors did not change groups at 5 (t120) or 10 (t240) days of imaging, demonstrating some stability in arbor complexity over time. (**G**) Correlation between minimum and maximum number of terminal branches for 26 receptive arbors observed every 12 h for 10 days.

Variability in arbor size over 10 days differs across arbors

Because arbor size (convex hull) was not heavily impacted by the retraction of single terminal branches we hypothesized that arbor size is maintained despite constant arbor remodeling. To determine if this was the case, we examined whether arbor size (convex hull and total arbor length) changed over 10 days. To perform comparisons across all timepoints within a 10 day period, we developed a semi-automated image analysis pipeline in MATLAB, called ArborTools, to segment arbors and quantify convex hull and total arbor length (Figure 6A). Reconstructions of each arbor were verified visually to confirm that the arbor and the reconstruction matched (Figure 6, cyan vs white). Arbors with too much background noise for automatic tracing were removed from analysis. The volume occupied by the arbor (convex hull) changed in the taste bud across 10 days. In general, convex hull changed along with total length (Figure 6C). These changes in size could be due to changes in height, or x or y width, or combinations of these changes (Figure 6D). For example, the illustrated arbor (Figure 6 A-C), increases in size occur due to an increase in Y-width from 0 to 12 hours, but dramatically increases in size between hour 228-240 due to concurrent increases X, Y width and height.

When examining the extent to which individual arbors displayed changes in size, we noticed that some arbors appear to be more variable (Figure 6D). We divided them into two groups based on the variability of their sizes over 10 days (Figure 6E, insert). Arbors appear to divide into those that vary little over time and remain small, and those that remodel more extensively (Figure 6E). Those that remodel more extensively are also larger on average over 10 days. These two groups could represent phases in a

remodeling cycle that extends beyond 10 days, or it could represent two distinct populations of taste arbors that differ is regard to degree of remodeling.

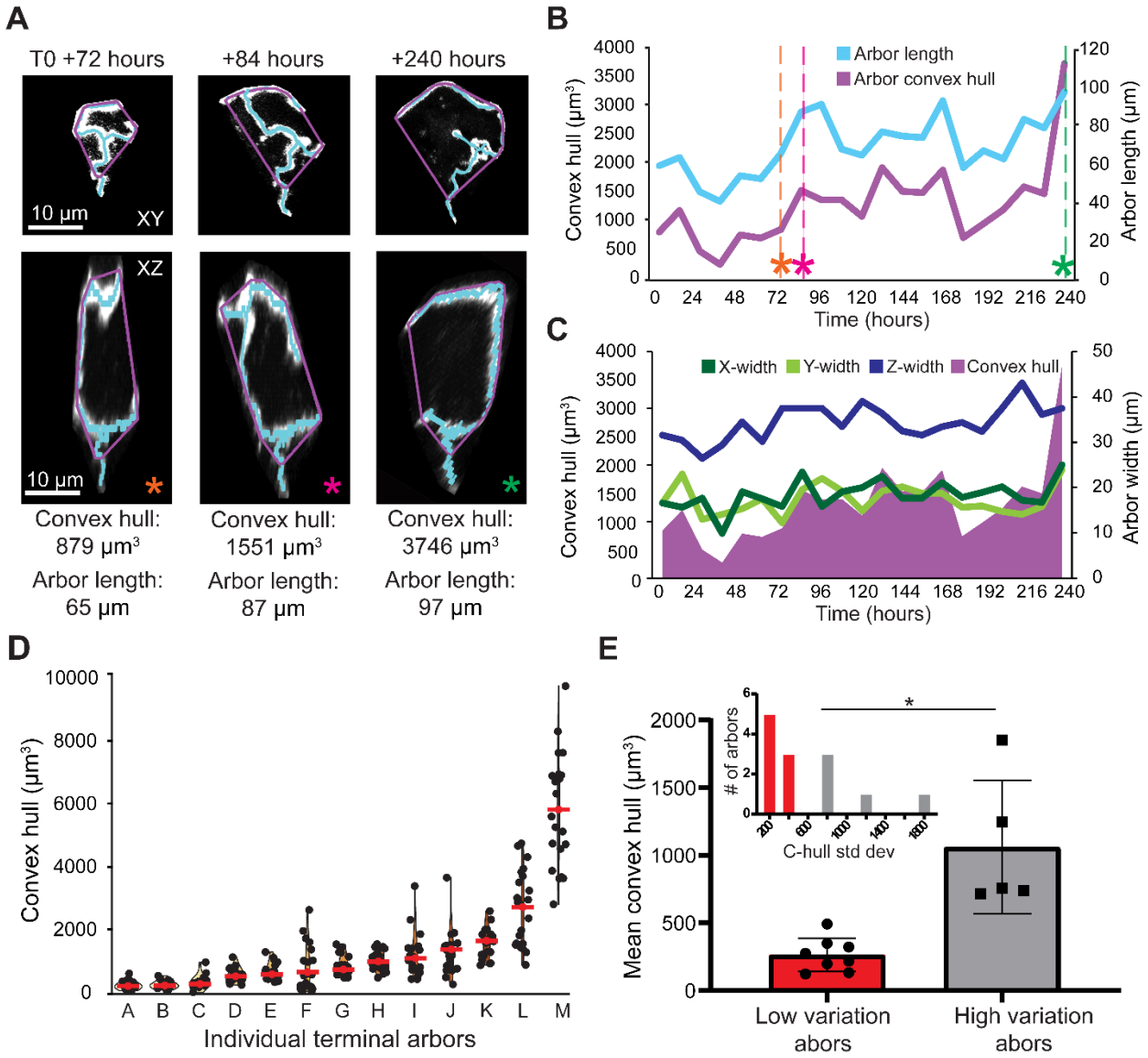

Figure 6. Taste neuron arbors vary in size over 10 days. A custom image analysis pipeline was developed to segment arbor structure from raw image TIF stacks. (**A**) Examples of convex hulls (purple) and arbor skeletons (cyan) generated from segmentation data are shown in two orientations and at three timepoints. Colored asterisks at each timepoint are used to indicate convex hull and arbor length in (C). (**B**) Convex hull size (purple line) and arbor length (cyan) for the example arbor in (A) are shown across the entire 10-day imaging window. **(C)** Convex hull potted with Z-height, x-width and y-width over time. (**D**) Convex hull measured for 13 individual arbors arranged by ascending average size. Average convex hull and arbor length during the 10-day imaging window are indicated with red dots and bars. **(E)** Within 10 days small arbors remodel little and are small, while other remodel more extensively and tend to be larger and more variant in size.

Number of arbors within a taste bud is stable over 100 days

Within 10-days, we did not observe any new arbors growing into taste buds, and only a small number of arbors were lost. Therefore, total number of arbors may be a stable feature for a given taste neuron over time. Alternatively, gain loss of whole arbors may occur, but require a longer time than 10 days. To distinguish between these possibilities, we imaged taste buds every 10 days for 60 or 100 days in mice where neurons were sparsely labeled. We observed taste buds with labeled arbors (n = 18 for 60 days, n = 13 for 100 days) as well as buds without labeled arbors (n = 18 for 60 days, n = 13 for 100 days) (Figure 7A). The arbor structure in the papillae core was largely unchanged over 100 days (Figure 7B, purple dotted line). In addition, no taste buds acquired new labeled arbors in 60 or 100 days of imaging. Initially, 18 taste buds contained a total of 33 labeled arbors. After 60 days of imaging, 31 arbors were still present. No additional labeled arbors were lost from the remaining taste buds throughout the 100 days (Figure 7C). These results suggest that the number of arbors is a stable feature of the neuron in adulthood. Arbors do not exhibit the full range of complexity over 100 days (Figure 7D). Convex hull and arbor length also indicate that some arbors remain small, while others are more variable (Figure 7E-F).

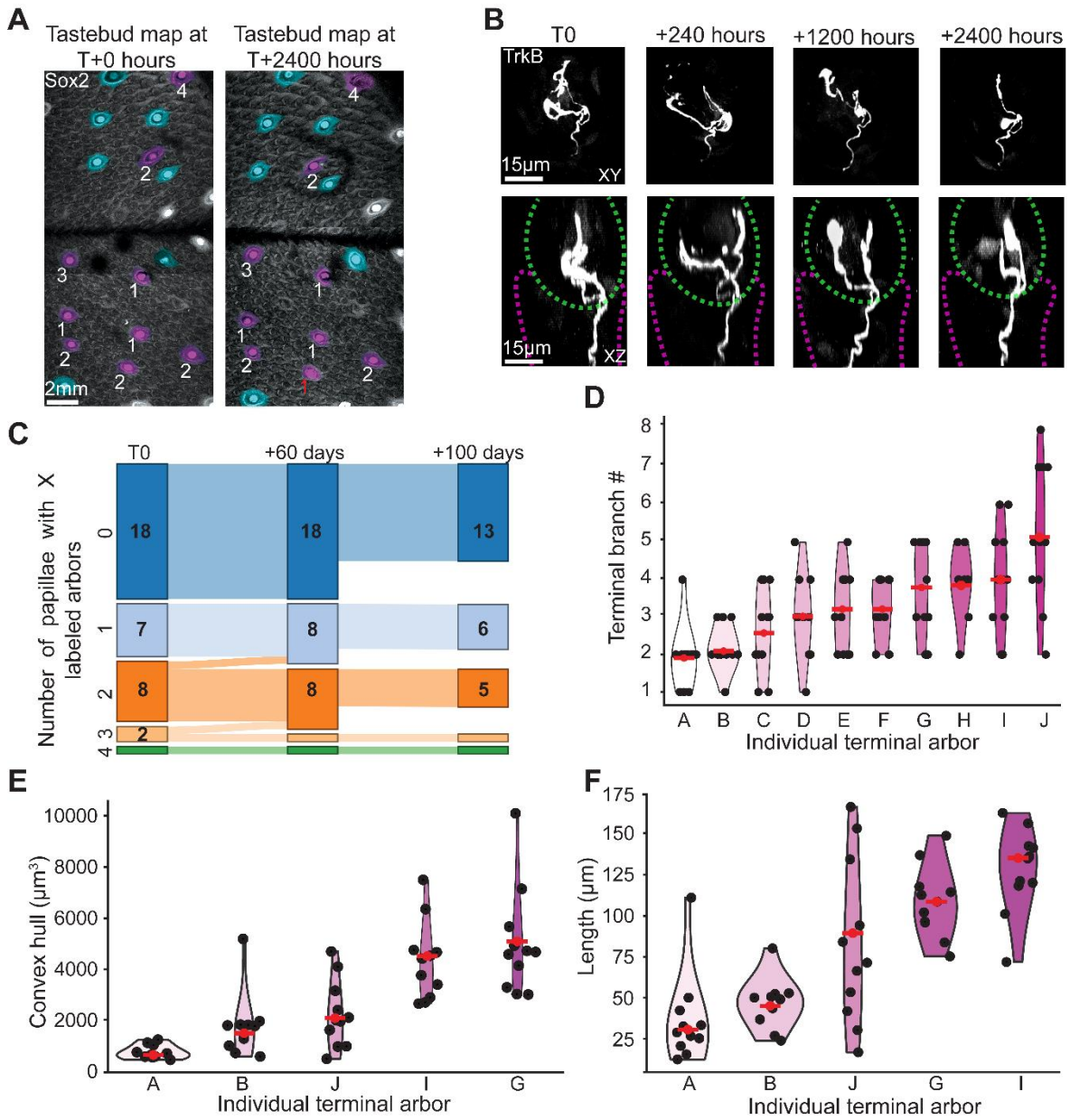

Figure 7. Arbor number is stable over 100 days. (**A**) Two papillae maps of the same regions shown 100 days apart. Purple taste buds contained labeled arbors (number of arbors labeled in white), and blue taste buds did not contain labeled arbors. One papilla in this map lost an arbor during the 100-day window (red label). (**B**) Example arbor at days 0, 10, 50, and 100. The taste bud is outlined in a green dotted line and papillae core in magenta. (**C**) Taste buds were categorized by number of labeled arbors and plotted in a Sankey diagram. No taste buds acquired new arbors, and two taste buds lost an arbor during the first 60 days. One mouse was not imaged past day 60. (**D**) Violin plots of terminal branch number for 10 arbors imaged every 10 days for 100 days. Average number of terminal branches during the 100-day window are indicated with red dots and bars. Violin plots of convex hull (**E**) and arbor length (**F**) for five individual arbors imaged every 10 days for 100 days. Arbor identities are conserved from (**D**).

Discussion

Taste bud cells are continuously replaced (Beidler and Smallman, 1965; Farbman, 1980; Hamamichi et al., 2006), but whether the arbors of taste neurons remodel while forming connections with these new taste bud cells is unknown. This makes it unclear whether the observed variation in peripheral taste neuron structure occurs because taste neurons exist as different morphological types or whether the variation is entirely due to plasticity (Huang et al., 2021). Here, we show for the first time that taste neurons exhibit structural remodeling. In taste buds, arbors form and retract terminal branches rapidly and continuously. This rate was much faster than predicted if branches were added to connect to new cells or lost to retract from old ones. Within an individual arbor growth is concurrent with retraction. Surprisingly, this plasticity is not impacted by manipulating cell turn over, suggesting that terminal branch loss and gain are intrinsic features of taste neurons. Lastly, the total number of arbors for a given taste neuron was stable over time. Thus, taste neurons constantly reconnect to new taste bud cells by having arbors capable of high-speed remodeling. However, they also maintain a stable number of arbors, such that differences in arbor number across neurons is due to an intrinsic feature of the neuron – dictated by neuron type.

Most arbors only connect to one taste bud cell at any given time (Kinnamon et al., 1988; Wilson et al., 2022). In a 10-day period roughly half of the population of taste bud cells turnover. Therefore, we anticipated that half the arbors sampled would lose their connection to a bud cell and/or gain a new connection within 10-days We expected that arbors would demonstrate periods of stability while connected to a taste bud cell, followed by remodeling when connections are broken (Ohman et al., submitted). This type of

phasic remodeling is observed in arbors of touch neurons that receive input from Merkel cells (Marshall et al., 2016). The results of our study do not support the model that taste neurons experience distinct phases of remodeling and stability; rather the arbors od taste neurons are continuously remodeling (Takahashi et al., 2019). We conclude that terminal branches are not formed to connect to taste bud cells nor lost because taste bud cells die.

Taste buds release growth and guidance factors, and these factors released from cells entering the taste bud could stimulate branch formation and/or growth of arbors (Donnelly et al., 2018; Lee et al., 2017; Meng et al., 2015; Nosrat et al., 2012; Treffy et al., 2016; Yee et al., 2003; Zeng and Sanes, 2017). However, our finding that terminal branch remodeling is much faster than expected based on the rate of cell turnover is not consistent with this possibility. Instead, terminal branch remodeling may be an intrinsic feature of the neuron, which occurs regardless of what external factors are present. To assess whether this remodeling is driven by an intrinsic mechanism, we examined remodeling of terminal arbors in taste buds in which new cell entry was blocked. Treatment with LDE225 inhibits the taste bud cell differentiation such that new taste bud cells do not enter the taste bud (Castillo-Azofeifa et al., 2017; Kumari et al., 2015). Surprisingly, we found that inhibition of new cell entry into taste buds does not influence the rate or magnitude of terminal branch loss or formation. In fact, we observed some remodeling even when the entire taste bud was lost after LDE225 treatment. This finding is consistent with the presence of growth associated protein-43 (GAP43) in the arbors following treatment with LDE225 (Donnelly et al., 2022). Collectively, these findings

support the model that remodeling is an intrinsic characteristic of peripheral taste neurons.

Although terminal branch remodeling is an intrinsic feature of peripheral taste neurons, this does not mean that the numerous trophic and tropic factors identified in the taste bud do not have a role in the process of reconnecting existing arbors to new bud cells (Lee et al., 2017; Meng et al., 2015). For example, each arbor may continuously sample the cellular environment of the taste bud by extending terminal branches. An intrinsic program of constant remodeling would permit taste arbors to detect signals in their immediate environment, perhaps permitting an arbor to compare spatial arrangements of taste cells. Furthermore, if a terminal arbor comes in contact with a cell, then this constant terminal branch remodeling would permit detection of surface molecules, such as protocadherins (Hirose et al., 2020). Thus, terminal branch remodeling may be related to the detection of molecular cues, rather than a response by peripheral taste neurons to molecular cues.

End bulbs have been described previously in taste buds (Zaidi et al., 2016). Here we extend this finding to demonstrate that these end bulbs are mostly retraction bulbs. Retraction bulbs and branch swellings occur in other systems both during development and following injury (Bishop et al., 2004; Erturk et al., 2007). These observations suggest that retraction occurs by atrophy of arbor branches and engulfment of neuronal debris by phagocytic cells. For motor neurons innervating the neuromuscular junction, there is evidence that the loss of signal from the target triggers the formation of retraction bulbs and the atrophy of the axon (Bernstein and Lichtman, 1999). While the anticipated source of such a signal in the taste bud would be from a connected taste bud cell, we observed

that much like terminal branch addition and loss, retraction events occurred much more frequently than would be predicted based on the loss of a connected taste-bud cell. Perhaps taste bud cell loss is much faster than predicted, or the trigger for terminal branch atrophy may not arise from an innervated cell.

Whereas terminal branches remodel at a surprisingly high rate, the gain and loss of terminal branches occurs concurrently such that loss of a terminal arbor does not reflect a decrease in arbor size. Remodeling in arbor size does occur, however the degree of plasticity in arbor size varies across individual arbors, with some changing size much more than others. We recently found that individual taste neurons either tend to have all small arbors, or have arbors that vary in size (Ohman et al., in submission). It may be that degree of plasticity in an arbor size varies across neurons and reflects different types of taste neurons. Larger arbors sizes with more plasticity could increase the probability of the neuron contacting a scarce taste bud cell type.

Interestingly, the number of arbors labeled remained stable over 100 days. The presence or absence of arbors in the bud is dictated by branch points within the axon that are outside the taste bud. This finding indicates that branches in the lamina propria and tongue muscle are not added and/or lost in adulthood. Even when taste buds are eliminated, individual arbors remain in the location previously occupied by taste buds. A taste neuron may have between 1 to 14 arbors (Huang et al., 2021). Given that most arbors only connect to 1-2 cells, the number of arbors determines how many taste bud cells provide input to a given neuron (Wilson et al., 2022). Neurons with more arbors are predicted to be both more sensitive and more broadly tuned than neurons with fewer arbors (Ohman and Krimm, 2021). Although there is evidence that peripheral taste

neurons can change function over time (Bradley et al., 1997), there is also likely some level of functional stability so that taste information is relayed to the brain as an interpretable code. Maintaining a constant number of arbors is one mechanism by which taste neurons could maintain functional stability over time.

We recently measured the morphology of taste neurons for the first time and divided them into four categories based on branching characteristics (Huang et al., 2021). Here, we determined that some of these morphologies are snapshots in time of continuously remodeling neurons, while others are not. Taste neurons could exist as morphological types based on stable features (number of taste buds innervated and number of arbors). These stable anatomical features of taste neurons could be a characteristic of specific taste neuron genetic types (Dvoryanchikov et al., 2017; Zhang et al., 2019) or functional differences (Barretto et al., 2015; Lundy and Contreras, 1999; Wu et al., 2015). It is yet to be determined if peripheral taste neuron types are defined by a combination of expression, function, and stable morphological features (Zeng and Sanes, 2017). By defining the stable versus unstable morphological features of gustatory neurons, this possibility can now be examined.

Materials and methods

Animals

All animals were cared for in accordance with guidelines set by the United States Public Health Service Policy on the Humane Care and Use of Laboratory Animals and the National Institutes of Health Guide for the Care and Use of Laboratory Animals.

TrkB^{CreER} mice (*Ntrk2*$^{tm3.1(cre/ERT2)Ddg}$; ; ISMR catalog #JAX:027214, RRID:IMSR_JAX:027214) were crossed with Cre-dependent tdTomato mice (Rutlin et al., 2014; RRID: IMSR_JAX:007914) to obtain *TrkB*^{CreER}:tdTomato mice in which tdTomato is expressed following TrkB-driven Cre-mediated gene recombination. These mice were crossed with a Sox2-GFP line (Sox2^{tm2Hoch};; ISMR catalog #JAX:017592, RRID:IMSR_JAX:017592). Phox2b-Cre mice (MRRC_034613-UCD) were also bred with tdTomato reporter mice for fixed tissue experiments. K14^{CreERT} mice; ISMR catalog #JAX:005107, RRID:IMSR_JAX:005107) were crossed with tdTomato reporter mice for lineage tracing of taste cells. For all experiments, mice were postnatal day 60 or older at the initial imaging session. Males and females were used across all *in vivo* experiments (24 males and 19 females in total). Mice were divided across experiments as follows: 10-day imaging (n = 5), 100-day imaging (n = 3). 4 h imaging (n = 5) 1 h imaging (n = 4), 6-h imaging (n = 2), 4 h live imaging Hh-inhibition (n = 6; vehicle n = 2, LDE225 n = 4), new cells entering the taste bud (n = 7; vehicle n = 2, LDE225 n = 5), confocal imaging experiments examining taste bud size (n = 10; vehicle n = 5, LDE225 n = 5).

Tamoxifen administration

Tamoxifen (T5648, MiliporeSigma, St. Louis, MO) was dissolved in corn oil (C-8267, MiliporeSigma) at 20 mg/ml by shaking and heating at 42°C and injected in a single dose on postnatal day 40 by intragastric gavage.

LDE225 administration

Mice were treated by daily oral gavage for 10, 16, or 23 days with vehicle (PEG 400:5% dextrose in water) or LDE225 (NVP-LDE225, ChemieTek, Indianapolis, IN)

dissolved in vehicle at a dose of 20 mg/kg. The dose was determined based on Kumari et al. (2015) and preliminary studies. The oral gavage probe (22-gauge, 25 mm; Instech) by-passed all oral tissues for direct delivery into the stomach.

Immunohistochemistry

Phox2b-Cre:tdTomato mice were killed by avertin overdose (4 mg/kg) and perfused transcardially with 4% paraformaldehyde. Dissected tissues were postfixed in 4% paraformaldehyde for 2 h (for thin serial sections) or overnight (thick sections and whole mounts), rinsed with PBS, and transferred to 30% sucrose at 4°C overnight. A razor blade was used to remove the anterior two-thirds of the tongue, after which tongues were carefully split down the midline with a razor blade under a dissection microscope. Tongues were frozen the next day in OCT and stored at -80°C before processing for whole-mount staining. Whole-mount immunohistochemistry of the lingual epithelium was performed to visualize innervated taste buds. First, the underlying muscle and lamina propria were removed as described previously (Ohman and Krimm, 2021). The isolated lingual epithelium was then washed for 15 min (three times) in 0.1 M PBS. Tissues were then incubated in blocking solution (3% donkey serum and 0.5% Triton X-100 in 0.1 M PBS) at 4°C overnight and then incubated for 5 days at 4°C with primary antibodies (DsRed (rabbit) and Troma1 (rat)) in antibody solution (0.5% Triton X-100 in 0.1 M PBS). Tissues were rinsed four times for 15 min each with 0.1 M PBS and incubated with secondary antibodies anti-DsRed (1:500; RRID:AB_10013483; Living Colors DsRed polyclonal; Takara Bio USA, San Jose, CA) and anti-Troma1 (1:500, Alexa Fluor 488 AffiniPure, RRID:AB_2340619; Jackson ImmunoResearch, West Grove, PA). Tissues

were then rinsed again, mounted with Fluoromount-G, and coverslipped (high precision, 0107242; Marienfeld).

Confocal imaging

Taste bud images were obtained using an Olympus Fluoview FV1000 confocal laser-scanning microscope with a 60× NA1.4 lens objective using a zoom of 3, Kalman 2. Image sizes were initially set at 1024 × 1024 pixels but were cropped to reduce scanning time and bleaching. Serial optical sections at intervals of 0.47 μm in the Z dimension were captured, which is the optimal size at 60× magnification for 3D reconstruction. All colors were imaged sequentially in separate channels to avoid bleed-through. Image stacks were then deconvolved using AutoQuant X3 software (Media Cybernetics, Rockville, MD) to reduce out-of-focus fluorescence and improve image quality.

Two-photon *in vivo* imaging

In vivo 2PLSM imaging was performed using a movable objective microscope (Sutter Instruments, Novato, CA). A Fidelity-2 1070-nm laser (Coherent, Silicon Valley was used to visualize tdTomato, and a Chameleon tunable laser (Coherent) set to 920 nm was used to visualize GFP. A custom-built tongue holder, based on a published design, was used to stabilize the anterior tongue for imaging of the dorsal surface (Han and Choi, 2018). Mice were anesthetized using a 0.6% isoflurane (Henry Schien, Melville, NY) and O_2 mixture. A temperature controller was used to monitor and maintain body temperature at 36°C. Ophthalmic lubricant ointment (Henry Schien) was applied to the eyes. Taste bud maps were acquired using a 10 × 0.3 numerical aperture water immersion objective lens (Carl Zeiss, USA), and images of receptive arbors were

acquired using a 40 × 10 numerical aperture water immersion lens (Zeiss). An early version of ScanImage (Matlab) was used to collect images. Receptive arbors were typically imaged to 70 microns in depth below the surface of the tongue, and 80 × 80 µm optical sections (512 × 512 pixels) were collected at 0.5 or 1 µm increments.

Image analysis

Taste bud volume was calculated by contouring whole-mount-stained taste buds at 3 micron increments perpendicular to the XY plane of the confocal z-stack. K14 cells were manually quantified from taste bud z-stacks using ImageJ. Terminal branches of sparsely labeled receptive arbors were manually quantified from z-stacks using ImageJ. Terminal branches that displayed retraction bulbs were quantified using the SNT plugin. A custom Matlab program (ArborTools, Github link to software will go here) was used to automatically segment arbors. 3D images stacks were cropped to isolate terminal arbors from background. A custom filter was used to extract initial segmentation volumes (Lang et al., 2011). After automatic segmentation, the segmented arbors were compared to the arbors and instances where background pixels were segmented were manually selected to not be included in the convex hull and length analysis. From segmented volumes skeletons were extracted using the Treestoolbox (Cuntz et al., 2010). All convex hull and arbor length data reported were generated from ArborTools.

Statistical analysis

Rates of terminal branch change were compared across image sets by first testing whether the measure was normally distributed using a Shapiro-Wilk test. If a measure was normally distributed, then differences were determined using a Student's t-test for

two groups or one-way analysis of variance with a Tukey *post hoc* test for more than two groups. If a measure was not normally distributed, then differences were determined using a Mann-Whitney test for two groups or Kruskal-Wallis test for more than two groups. A p-value <0.05 was used to determine statistical significance.

References

Anderson CB, Larson ED. 2019. Single Cell Transcriptional Profiling of Phox2b-Expressing Geniculate Ganglion Neurons (preprint). Neuroscience. doi:10.1101/812578

AU - Ohman LC, AU - Krimm RF. 2021. Whole-Mount Staining, Visualization, and Analysis of Fungiform, Circumvallate, and Palate Taste Buds. *J Vis Exp* e62126. doi:10.3791/62126

Barretto RPJ, Gillis-Smith S, Chandrashekar J, Yarmolinsky DA, Schnitzer MJ, Ryba NJP, Zuker CS. 2015. The neural representation of taste quality at the periphery. *Nature* **517**:373–376. doi:10.1038/nature13873

Beidler LM, Smallman RL. 1965. RENEWAL OF CELLS WITHIN TASTE BUDS. *J Cell Biol* **27**:263–272. doi:10.1083/jcb.27.2.263

Bernstein M, Lichtman JW. 1999. Axonal atrophy: The retraction reaction. *Curr Opin Neurobiol* **9**:364–370. doi:10.1016/S0959-4388(99)80053-1

Bishop DL, Misgeld T, Walsh MK, Gan W-B, Lichtman JW. 2004. Axon Branch Removal at Developing Synapses by Axosome Shedding. *Neuron* **44**:651–661. doi:10.1016/j.neuron.2004.10.026

Bradley RM, Cao X, Akin T, Najafi K. 1997. Long term chronic recordings from peripheral sensory fibers using a sieve electrode array. *J Neurosci Methods* **73**:177–186. doi:10.1016/S0165-0270(97)02225-5

Castillo D, Seidel K, Salcedo E, Ahn C, de Sauvage FJ, Klein OD, Barlow LA. 2014. Induction of ectopic taste buds by SHH reveals the competency and plasticity of adult lingual epithelium. *Development* **141**:2993–3002. doi:10.1242/dev.107631

Castillo-Azofeifa D, Losacco JT, Salcedo E, Golden EJ, Finger TE, Barlow LA. 2017. Sonic hedgehog from both nerves and epithelium is a key trophic factor for taste bud maintenance. *Development* **144**:3054–3065. doi:10.1242/dev.150342

Cuntz H, Forstner F, Borst A, Häusser M. 2010. One Rule to Grow Them All: A General Theory of Neuronal Branching and Its Practical Application. *PLoS Comput Biol* **6**:e1000877. doi:10.1371/journal.pcbi.1000877

Donnelly CR, Kumari A, Li L, Vesela I, Bradley RM, Mistretta CM, Pierchala BA. 2022. Probing the multimodal fungiform papilla: complex peripheral nerve endings of chorda tympani taste and mechanosensitive fibers before and after Hedgehog pathway inhibition. *Cell Tissue Res* **387**:225–247. doi:10.1007/s00441-021-03561-1

Donnelly CR, Shah AA, Mistretta CM, Bradley RM, Pierchala BA. 2018. Biphasic functions for the GDNF-Ret signaling pathway in chemosensory neuron development and diversification. *Proc Natl Acad Sci* **115**. doi:10.1073/pnas.1708838115

553 Dvoryanchikov G, Hernandez D, Roebber JK, Hill DL, Roper SD, Chaudhari N. 2017. Transcriptomes and
554 neurotransmitter profiles of classes of gustatory and somatosensory neurons in the geniculate
555 ganglion. *Nat Commun* **8**. doi:10.1038/s41467-017-01095-1
556 Ermilov AN, Kumari A, Li L, Joiner AM, Grachtchouk MA, Allen BL, Dlugosz AA, Mistretta CM. 2016.
557 Maintenance of Taste Organs Is Strictly Dependent on Epithelial Hedgehog/GLI Signaling. *PLOS*
558 *Genet* **12**:e1006442. doi:10.1371/journal.pgen.1006442
559 Erturk A, Hellal F, Enes J, Bradke F. 2007. Disorganized Microtubules Underlie the Formation of
560 Retraction Bulbs and the Failure of Axonal Regeneration. *J Neurosci* **27**:9169–9180.
561 doi:10.1523/JNEUROSCI.0612-07.2007
562 Farbman AI. 1980. RENEWAL OF TASTE BUD CELLS IN RAT CIRCUMVALLATE PAPILLAE. *Cell Prolif* **13**:349–
563 357. doi:10.1111/j.1365-2184.1980.tb00474.x
564 Hamamichi R, Asano-Miyoshi M, Emori Y. 2006. Taste bud contains both short-lived and long-lived cell
565 populations. *Neuroscience* **141**:2129–2138. doi:10.1016/j.neuroscience.2006.05.061
566 Han J, Choi M. 2018. Comprehensive functional screening of taste sensation *in vivo* (preprint).
567 Neuroscience. doi:10.1101/371682
568 Hirose F, Takai S, Takahashi I, Shigemura N. 2020. Expression of protocadherin-20 in mouse taste buds.
569 *Sci Rep* **10**:2051. doi:10.1038/s41598-020-58991-8
570 Huang T, Ohman LC, Clements AV, Whiddon ZD, Krimm RF. 2021. Variable Branching Characteristics of
571 Peripheral Taste Neurons Indicates Differential Convergence. *J Neurosci* **41**:4850.
572 doi:10.1523/JNEUROSCI.1935-20.2021
573 Jacobsen AA, Aldahan AS, Hughes OB, Shah VV, Strasswimmer J. 2016. Hedgehog Pathway Inhibitor
574 Therapy for Locally Advanced and Metastatic Basal Cell Carcinoma: A Systematic Review and
575 Pooled Analysis of Interventional Studies. *JAMA Dermatol* **152**:816.
576 doi:10.1001/jamadermatol.2016.0780
577 Kinnamon JC, Sherman TA, Roper SD. 1988. Ultrastructure of mouse vallate taste buds: III. Patterns of
578 synaptic connectivity. *J Comp Neurol* **270**:1–10. doi:10.1002/cne.902700102
579 Kumari A, Ermilov AN, Allen BL, Bradley RM, Dlugosz AA, Mistretta CM. 2015. Hedgehog pathway
580 blockade with the cancer drug LDE225 disrupts taste organs and taste sensation. *J Neurophysiol*
581 **113**:1034–1040. doi:10.1152/jn.00822.2014
582 Kumari A, Ermilov AN, Grachtchouk M, Dlugosz AA, Allen BL, Bradley RM, Mistretta CM. 2017. Recovery
583 of taste organs and sensory function after severe loss from Hedgehog/Smoothened inhibition
584 with cancer drug sonidegib. *Proc Natl Acad Sci* **114**:E10369–E10378.
585 doi:10.1073/pnas.1712881114
586 Lacouture ME, Dréno B, Ascierto PA, Dummer R, Basset-Seguin N, Fife K, Ernst S, Licitra L, Neves RI, Peris
587 K, Puig S, Sokolof J, Sekulic A, Hauschild A, Kunstfeld R. 2016. Characterization and Management
588 of Hedgehog Pathway Inhibitor-Related Adverse Events in Patients With Advanced Basal Cell
589 Carcinoma. *The Oncologist* **21**:1218–1229. doi:10.1634/theoncologist.2016-0186
590 Lang S, Drouvelis P, Tafaj E, Bastian P, Sakmann B. 2011. Fast extraction of neuron morphologies from
591 large-scale SBFSEM image stacks. *J Comput Neurosci* **31**:533–545. doi:10.1007/s10827-011-
592 0316-1
593 Lee H, Macpherson LJ, Parada CA, Zuker CS, Ryba NJP. 2017. Rewiring the taste system. *Nature* **548**:330–
594 333. doi:10.1038/nature23299
595 Liebl DJ, Mbiene J-P, Parada LF. 1999. NT4/5 Mutant Mice Have Deficiency in Gustatory Papillae and
596 Taste Bud Formation. *Dev Biol* **213**:378–389. doi:10.1006/dbio.1999.9385
597 Lindemann B. 2001. Receptors and transduction in taste. *Nature* **413**:219–225. doi:10.1038/35093032
598 Lu W-J, Mann RK, Nguyen A, Bi T, Silverstein M, Tang JY, Chen X, Beachy PA. 2018. Neuronal delivery of
599 Hedgehog directs spatial patterning of taste organ regeneration. *Proc Natl Acad Sci* **115**:E200–
600 E209. doi:10.1073/pnas.1719109115

601 Lundy RF, Contreras RJ. 1999. Gustatory Neuron Types in Rat Geniculate Ganglion. *J Neurophysiol*
602 **82**:2970–2988. doi:10.1152/jn.1999.82.6.2970
603 Marshall KL, Clary RC, Baba Y, Orlowsky RL, Gerling GJ, Lumpkin EA. 2016. Touch Receptors Undergo
604 Rapid Remodeling in Healthy Skin. *Cell Rep* **17**:1719–1727. doi:10.1016/j.celrep.2016.10.034
605 Meng L, Ohman-Gault L, Ma L, Krimm RF. 2015. Taste Bud-Derived BDNF Is Required to Maintain Normal
606 Amounts of Innervation to Adult Taste Buds. *eneuro* **2**:ENEURO.0097-15.2015.
607 doi:10.1523/ENEURO.0097-15.2015
608 Miller IJ, Reedy FE. 1990. Variations in human taste bud density and taste intensity perception. *Physiol*
609 *Behav* **47**:1213–1219. doi:10.1016/0031-9384(90)90374-D
610 Nosrat IV, Margolskee RF, Nosrat CA. 2012. Targeted Taste Cell-specific Overexpression of Brain-derived
611 Neurotrophic Factor in Adult Taste Buds Elevates Phosphorylated TrkB Protein Levels in Taste
612 Cells, Increases Taste Bud Size, and Promotes Gustatory Innervation. *J Biol Chem* **287**:16791–
613 16800. doi:10.1074/jbc.M111.328476
614 Ohman LC, Hanbala L, Krimm RF. in submission. Taste arbor structural variability analyzed across taste
615 regions.
616 Ohman LC, Krimm RF. 2021. Variation in taste ganglion neuron morphology: insights into taste function
617 and plasticity. *Curr Opin Physiol* **20**:134–139. doi:10.1016/j.cophys.2020.12.011
618 Ohman-Gault L, Huang T, Krimm R. 2017. The transcription factor Phox2b distinguishes between oral
619 and non-oral sensory neurons in the geniculate ganglion. *J Comp Neurol* **525**:3935–3950.
620 doi:10.1002/cne.24312
621 Okubo T, Pevny LH, Hogan BLM. 2006. Sox2 is required for development of taste bud sensory cells.
622 *Genes Dev* **20**:2654–2659. doi:10.1101/gad.1457106
623 Patel AV, Krimm RF. 2010. BDNF is required for the survival of differentiated geniculate ganglion
624 neurons. *Dev Biol* **340**:419–429. doi:10.1016/j.ydbio.2010.01.024
625 Romanov RA, Lasher RS, High B, Savidge LE, Lawson A, Rogachevskaja OA, Zhao H, Rogachevsky VV,
626 Bystrova MF, Churbanov GD, Adameyko I, Harkany T, Yang R, Kidd GJ, Marambaud P, Kinnamon
627 JC, Kolesnikov SS, Finger TE. 2018. Chemical synapses without synaptic vesicles: Purinergic
628 neurotransmission through a CALHM1 channel-mitochondrial signaling complex. *Sci Signal*
629 **11**:eaao1815. doi:10.1126/scisignal.aao1815
630 Takahashi S, Ishida A, Kubo A, Kawasaki H, Ochiai S, Nakayama M, Koseki H, Amagai M, Okada T. 2019.
631 Homeostatic pruning and activity of epidermal nerves are dysregulated in barrier-impaired skin
632 during chronic itch development. *Sci Rep* **9**:8625. doi:10.1038/s41598-019-44866-0
633 Tang JY, Mackay-Wiggan JM, Aszterbaum M, Yauch RL, Lindgren J, Chang K, Coppola C, Chanana AM,
634 Marji J, Bickers DR, Epstein EH. 2012. Inhibiting the Hedgehog Pathway in Patients with the
635 Basal-Cell Nevus Syndrome. *N Engl J Med* **366**:2180–2188. doi:10.1056/NEJMoa1113538
636 Treffy RW, Collins D, Hoshino N, Ton S, Katsevman GA, Oleksiak M, Runge EM, Cho D, Russo M, Spec A,
637 Gomulka J, Henkemeyer M, Rochlin MW. 2016. Ephrin-B/EphB Signaling Is Required for Normal
638 Innervation of Lingual Gustatory Papillae. *Dev Neurosci* **38**:124–138. doi:10.1159/000444748
639 Vandenbeuch A, Larson ED, Anderson CB, Smith SA, Ford AP, Finger TE, Kinnamon SC. 2015. Postsynaptic
640 P2X3-containing receptors in gustatory nerve fibres mediate responses to all taste qualities in
641 mice: Role of P2X3-containing receptors in taste. *J Physiol* **593**:1113–1125.
642 doi:10.1113/jphysiol.2014.281014
643 Wilson CE, Lasher RS, Yang R, Dzowo Y, Kinnamon JC, Finger TE. 2022. Taste Bud Connectome:
644 Implications for Taste Information Processing. *J Neurosci* **42**:804. doi:10.1523/JNEUROSCI.0838-
645 21.2021
646 Wu A, Dvoryanchikov G, Pereira E, Chaudhari N, Roper SD. 2015. Breadth of tuning in taste afferent
647 neurons varies with stimulus strength. *Nat Commun* **6**:1–11.

Yarmolinsky DA, Zuker CS, Ryba NJP. 2009. Common Sense about Taste: From Mammals to Insects. *Cell* **139**:234–244. doi:10.1016/j.cell.2009.10.001

Yee CL, Jones KR, Finger TE. 2003. Brain-derived neurotrophic factor is present in adult mouse taste cells with synapses. *J Comp Neurol* **459**:15–24. doi:10.1002/cne.10589

Zaidi FN, Cicchini V, Kaufman D, Ko E, Ko A, Van Tassel H, Whitehead MC. 2016. Innervation of taste buds revealed with Brainbow-labeling in mouse. *J Anat* **229**:778–790. doi:10.1111/joa.12527

Zaidi FN, Whitehead MC. 2006. Discrete Innervation of Murine Taste Buds by Peripheral Taste Neurons. *J Neurosci* **26**:8243–8253. doi:10.1523/JNEUROSCI.5142-05.2006

Zeng H, Sanes JR. 2017. Neuronal cell-type classification: challenges, opportunities and the path forward. *Nat Rev Neurosci* **18**:530–546. doi:10.1038/nrn.2017.85

Zhang J, Jin H, Zhang W, Ding C, O'Keeffe S, Ye M, Zuker CS. 2019. Sour Sensing from the Tongue to the Brain. *Cell* **179**:392-402.e15. doi:10.1016/j.cell.2019.08.031